Elliptical tubes receivers' efficiency analysis in solar power towers

Cite as: AIP Conference Proceedings **2126**, 030031 (2019); https://doi.org/10.1063/1.5117543
Published Online: 26 July 2019

Marta Laporte-Azcué, María de los Reyes Rodríguez-Sánchez and Domingo Santana

Elliptical Tubes Receivers' Efficiency Analysis in Solar Power Towers

Marta Laporte-Azcué[1, a)], María de los Reyes Rodríguez-Sánchez[1] and Domingo Santana[1]

[1]*Energy Systems Engineering Group (ISE). Department of Thermal and Fluid Engineering, University Carlos III of Madrid. Av. Universidad 30, 28911, Leganés, Madrid (Spain).*

[a)]Corresponding author: mlaporte@ing.uc3m.es

Abstract. The high costs of the heliostat field, as well as the issues related with the receiver operation in solar power towers are some of the main reasons to study different tube geometry shapes for the receiver. The new geometries intend to improve its thermal efficiency and increase its lifetime, such as the elliptical tubes presented in this research. A thermal model considering circumferential and longitudinal divisions of the tubes has been used to study the thermal efficiency of elliptical tubes receiver. For this analysis, the tube's geometry varies according to three different considerations when its major axis increases, and the resulting efficiencies are compared with the ones obtained for circular tubes of a fixed diameter. The results show that there is an improvement in the efficiency with the new tubes, because of the radiative exchange with the environment using the elliptical tubes, resulting in lesser radiative heat losses.

INTRODUCTION

The increasing concern about environmental issues and the scarcity of fossil resources have fuelled the interest in developing alternatives for electricity production using renewable energy sources. Concentrated solar power (CSP) energy, such as the one used in solar power tower (SPT) plants, is one of the most promising options to achieve said purpose.

These plants, using molten salts as working fluid, present the great benefit of being able to adapt their production to the electricity demand, taking advantage of their great thermal storage capacity to produce electricity steadily and stably. Three main subsystems can be distinguished in SPT plants: a mirrors field, called heliostats, the receiver, and the power block. The heliostats, that surround the receiver placed in the top of a tower, use a tracking system to successfully reflect and concentrate the direct solar radiation on the receiver's surface, radiation that it is converted in thermal power in the working fluid going through the receiver's tubes. Finally, the power block transforms such thermal energy in electricity.

However, this technology entails a great capital investment. It is estimated that the heliostats field and the receiver are responsible of around the 38% of the infrastructure costs [1]. This remarks the importance of operating with the maximum efficiency; an increase in the receiver's thermal efficiency would allow a more exact heliostat field sizing, preventing the infrastructure cost to increase unnecessarily. Besides, the receiver is the most restrictive subsystem of these plants, given that the high cycling temperatures that the tubes have to withstand led to stresses and fatigue and favour the corrosive effects of the molten salts at high temperature.

A vast variety of analyses about the receiver's design characteristics have already been carried out in previous works. These focus on aspects such as the diameter and the thickness of the tubes that form the receiver [2-4]. There has also been interest in studying the working fluid through the tubes [2,5] as well as its velocity [2], being even proposed the design of a new receiver design with variable working fluid velocity along each panel [6]. Other characteristics analysed are the number of panels of the receiver [3] or the tubes' material [4,7], considering among the possible options from nickel alloys (625LCF, 625, C4, 230, 617LCF and Haynes 230) to austenitic stainless steels

SolarPACES 2018
AIP Conf. Proc. 2126, 030031-1–030031-8; https://doi.org/10.1063/1.5117543
Published by AIP Publishing. 978-0-7354-1866-0/$30.00

(800H). Different tube diameters coexisting in a same panel have been studied [8], as well as the inclusion of different modifications on the circular cross-section tubes and new geometries that could substitute them, such as the spiral shaped tubes [9], a set of hexagonal-pyramid shaped elements [10], a reflector and a heating pipe coupled to the circular tubes, being the reflector and the heating pipe the ones that receive the direct radiation instead of the tubes [11], or the so-called bayonet tubes [12].

In this study it is proposed a new receiver configuration for SPTs, using elliptical tubes [13] instead of the traditional circular ones. To improve the thermal behaviour of the receiver, three different geometry configurations for the elliptical tubes' cross-section are considered, maintaining the same panel width:

- The first one keeps the number of tubes the same by having the minor axis length constant and equal to the circular tube diameter (constant minor axis, CMA)
- The second one presents the same cross flow than the circular tube (constant cross-section, CCS)
- The third one has the same outer perimeter than the circular tube, so the irradiation exchanged is equivalent (constant outer perimeter, COP)

It is also important to note that the geometry of the cross-section of the new tubes results in a greater moment of inertia when comparing it to the corresponding circular cross-section, reducing its bending due to thermal gradient [14] as well as the reaction forces caused by the clips that guide the tubes along the panel which, since they are welded to the tubes, are stress concentration points, being three times greater –in circular tubes- than the ones that appear in non-mechanically restricted tubes [15].

CENTRAL SOLAR RECEIVER CHARACTERISTICS

For this analysis an external tubular receiver has been considered, being placed on the top of a 120 m high tower. The receiver is a cylinder of 8.4 m of diameter covered with a white ceramic paint of high reflectivity [16] in order to decrease the radiation losses in the rear side of the tubes (the cylinder acts as a refractory wall, called rear wall as well). Surrounding the cylinder, 18 identical panels are placed, Fig 1(a), which are integrated by elliptical tubes, Fig 1(b), with their major axis facing the heliostats field, as well as their correspondent inlet and outlet collectors.

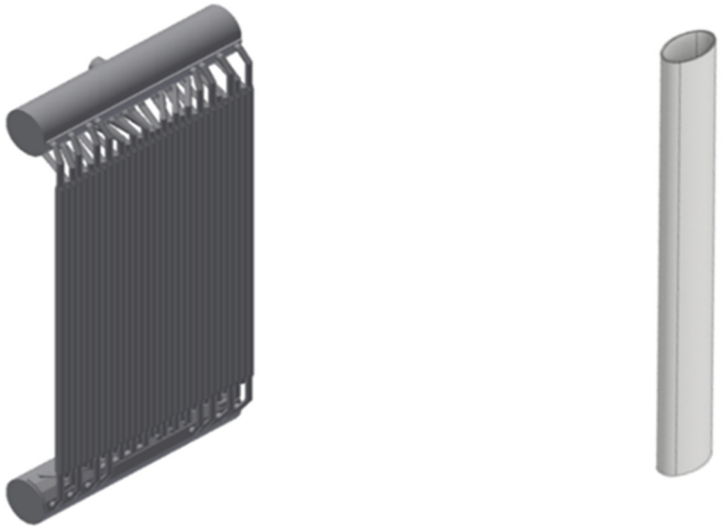

(a) (b)

FIGURE 1. (a) Representation of one of the receiver's panels, with its tubes and inlet and outlet collectors. (b) Vertical section of one of the panels' tubes.

Tubes, 10 m long, are presented in the three configurations summarized in Table 1. In order to be able to study the evolution of their thermal efficiency with their major axis, the latter will vary its length from the value corresponding to the diameter of the circular tube (4.22 cm) to the one that results in a 2:1 axis ratio for the first case (constant minor

axis), and for the other two cases as long as the minor axis doesn't result in a value less than 2.24 cm, a value that has been considered as limiting. The thickness is constant and equal to 1.65 mm in all the cases.

TABLE 1. Characteristics of the study cases.

Constant parameter	Major axis range (Lp)	Minor axis (Ls)	Limitation
Minor axis (CMA)	4.22 – 8.44 cm	4.22 cm	2:1 axis ratio
Cross section (CCS)	4.22 – 8 cm	$Ls = 4 \cdot area/\pi \cdot (Lp - 2 \cdot thick)$	Ls of 2.24 cm
Outer perimeter (COP)	4.22 – 5.52 cm	$Ls = \sqrt{8 \cdot (perimeter/2 \cdot \pi)^2 - Lp^2}$	Ls of 2.24 cm

The separation between tubes considered initially is the 8% the diameter length of the circular tube, although once it has been used to obtain the integer number of tubes per panel, such separation is recalculated taking into account the rounded result of the number of tubes. Also, the tubes are covered with black Pyromark, with solar effective absorptivity of 95% and infrared emissivity, temperature dependant [16].

The axial displacement of these tubes is restricted only in their upper end, allowing their free thermal extension. The tubes are guided by a series of clips placed periodically every 2 m along the whole length of the tubes to avoid their excessive bending, allowing in the points they are placed axial expansion but not flexion.

The tubes are manufactured from Inconel 625LCF, with a limiting film temperature of 630ºC [17] that depends on the heat transfer fluid (HTF) used, which is solar salt. This is the most used working fluid in SPT plants, which properties vary linearly with the temperature, being the main ones presented graphically in [18] and tabulated in [16]. The minimum inlet temperature of the salt must be 290°C to avoid its freezing and the maximum outlet temperature is 565°C to avoid its decomposition. Looking at the conclusions reached in [19], the HTF is divided into two parallel path flows, symmetrical with respect to the N-S axis, in which, in the north hemisphere, the HTF enters through the lower end of the panel facing north for each path, entering the following panel from its upper end, and so on, alternating its flowing direction panel after panel like a serpentine, and presenting a flow path cross after the sixth panel. To carry out this analysis, the design point is the solar-noon of the spring equinox at Seville, Spain.

THERMAL MODEL

The heat flux distribution on the receiver surface is two-dimensional, and it is considered to be almost homogeneous, using a multi aiming strategy [20], with an average flux of 0.472 MW/m^2 and a peak flux of 0.76 MW/m^2.

The receiver thermal model presented in [3] has been used to characterize the new receiver design. This model divides the tubes in circumferential and vertical cells, allowing a more precise prediction of the maximum tube's wall temperatures and providing a much more appropriate receiver's characterization than the models that only consider vertical divisions; circumferential cells are crucial to estimate the radiative losses, while the vertical cells are chosen as large as possible (0.5 m in this case) to minimize the error in that estimation, derived from the bidimensional view factors used. The resolution with the model selected is an iterative process in which it is assumed as initial hypothesis a homogeneous temperature in the whole tube, which will be recalculated iteratively, and a mass flow that will be modified until the inlet and outlet temperature requirements for the salt are met.

According to the results of [21], for the elliptical tubes studied, the Reynolds and Nusselt numbers can be obtained in the thermal model using the equivalent diameters of these tubes (internal and external). The axis ratios selected for the elliptical tubes have proven to provide valid results when comparing them to the ones obtained with the corresponding circular tubes. Also note than the Nusselt number has been calculated using the Gnielinski correlation, using the Darcy factor obtained with Petukhov correlation for smooth pipes.

In this model, just one representative tube per panel is studied. This is because all of the tubes in the same panel are assumed to behave likewise when it comes to the wall temperature distribution, given that they all receive the same radiation flux and the working fluid finds itself having the same temperature distribution in all of them. However, the adjacent tubes of the panel are indeed taken into account when calculating the radiative interaction of the tubes. Being that the tubes are symmetrical, the study tube will be understood just as two semi-tubes facing each other, Fig 2. The view factors allow to analyze the interaction among the three surfaces reflecting and intercepting radiation from the heliostats: tubes, rear wall and sky. The heliostats radiate directly to the tubes and the rear wall, the tubes reflect to all

the surfaces mentioned in a higher or lesser amount, depending on their geometry, and the rear wall has interaction with the sky and the tubes, Fig 2. In this case, Hottel's crossed-string method [22] can be easily applied by representing the elliptical cross sections as ovals, studying the interaction among the different circular sections that constitute them.

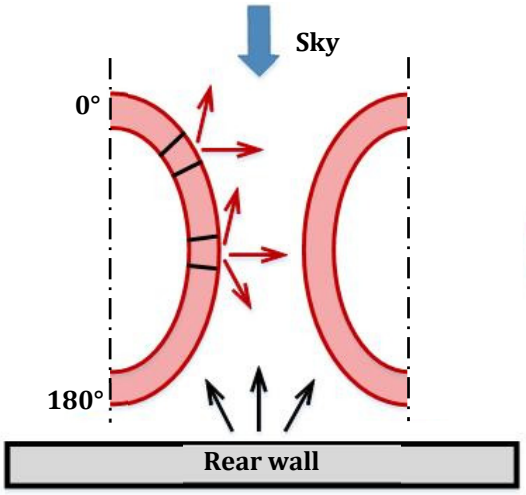

FIGURE 2. Simplified geometry that schematizes the radiative Exchange among the different surfaces involved.

RESULTS

Receiver's thermal efficiency, that involves the heat absorbed by the HTF and the reflected by the heliostats has been studied varying the major axis of the tubes, taking the circular tube of 4.22 cm of diameter as the starting point. Opposite to the 78.47% efficiency obtained with circular tubes, for the three of the elliptical configurations there is an improvement in the efficiency, Fig. 3, which increases with the major axis, reaching an optimum point and then decreasing from there. CCS and COP cases are the ones that reach the highest efficiency.

In the CCS and COP cases, the increase of the major axis comes with the decrease of the minor one. Thus, for the smallest values of the major axis, there is an initial number of tubes per panel, but reached certain major axis, the minor axis becomes such that allows an additional tube in the panel. Taking this into account, it was understandable that the results for these two cases presented peaks, like a saw, instead of being smooth curves like the CMA case. In Figure 3, and in the ones that follow and required it, only the peaks of efficiency for every range of axis ratios that resulted in the same number of tubes per panel have been represented. Such peaks of efficiency always belong to the last axis ratio that results in a certain number of tubes (therefore, the next major axis gives a greater number of tubes per panel, becoming the first one of its "range" of major axis for a certain number of tubes, and so on).

Figure 3 and successive figures include vertical lines that represent the tube diameter that reached the maximum film temperature for each case. The valid axis ratios are placed at the left of the corresponding line for each study case (4.84 cm for CMA, 5 cm for CCs and 5.08 cm for COP), since they reach a lower film temperature. However, the results of a bigger range of major axis have been included in all the Figures to illustrate better the tube's behaviour. Notice that the tube configurations that meet the film temperature condition are not the most efficient in each case, but these are the values that should be considered and not the ones surpassing the thermal limit. Among the valid results, the highest efficiency in each scenario is: 78.64 % with a major axis of 4.84 cm in the CMA case, 79.02% for a major axis of 5 cm in the CCS case, and 79.19% for a major axis of 5.08 in the COP case, while in the circular case the efficiency was 78.47%. This results in axis ratios of 1.147, 1.4 and 1.632 respectively; therefore, the optimum efficiency becomes higher with the axis ratio.

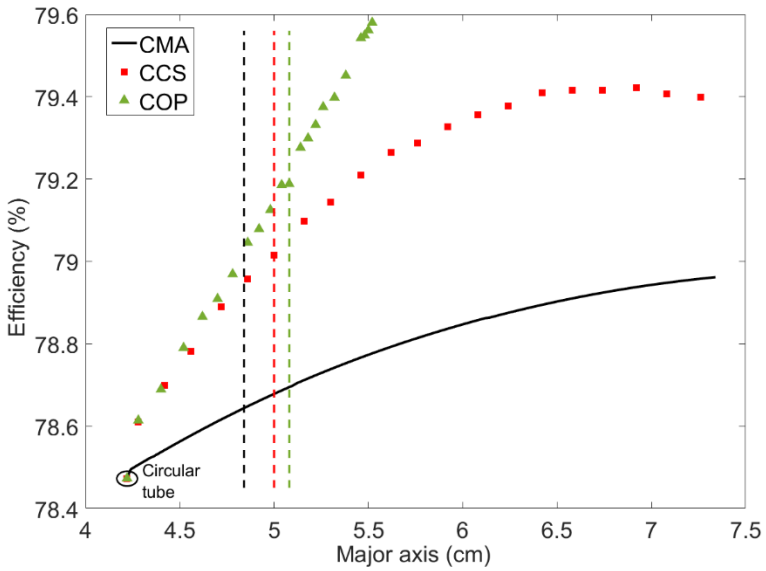

FIGURE 3. Receiver's thermal efficiency vs tube's major axis.

The improvement of the receiver's thermal efficiency can be explained with the view factors characteristic of the tube's geometry, being represented in Figure 4 the corresponding to the circumferential divisions of the circular tube's outer surface as well as the ones for the three optimum elliptical tubes, one for each study case.

Figure 4 goes from 0º at the front side of the tubes, the side facing the sun, to 180º at the rear side, omitting the whole contour given that it is a symmetric radiative surface, in shape itself and regarding the surfaces that interacts with. As it can be noticed, the more pointed is the ellipse (this is, the greater the axis ratio is), the cells of the tube that see the sun, being the latter placed at 0º, have lesser interaction with the sky than the ones of the circular tube, allowing the elliptical configurations to reflect a greater fraction of radiation to the opposite tube, favouring the decrease of the heat losses due to radiation.

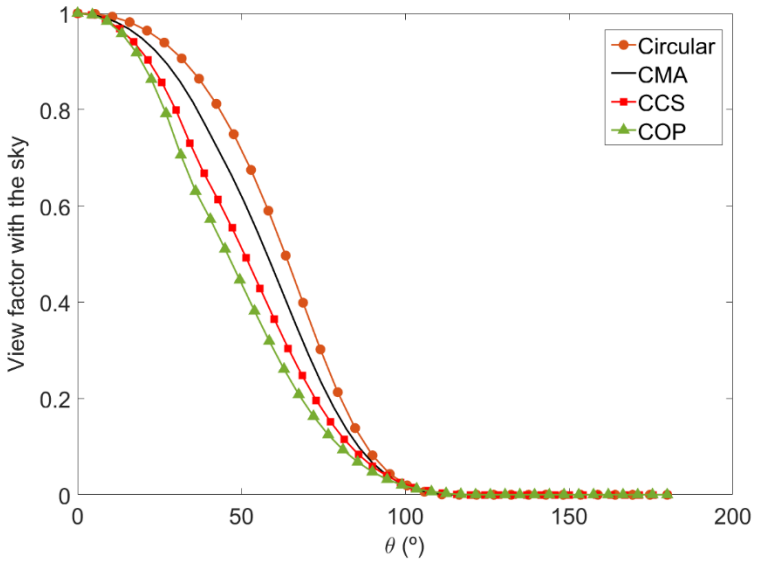

FIGURE 4. View factor of the tube with the sky, for the circular case and the optimum elliptical configuration in each of the three cases.

When it comes to the temperature of the tube's wall, it evolves practically in the same way for the three elliptical instances, being slightly lesser in the CCS and COP cases. The maximum wall temperature is presented in Figure 5 and it corresponds to the temperature in the front side of the tubes (0º). The increasing tendency of this temperature is due to the decrease of the salts' heat transfer coefficient with the increase of the major axis, reducing the heat transfer from the tubes to the salts and therefore, keeping the tubes hotter; such deterioration of the heat transfer coefficient occurs in the CMA case due to the increase of the cross section with the mayor axis, reducing fluid's velocity, and in the CCS and COP cases due to the increase of the number of tubes -which happens because when the major axis becomes greater, the minor one does the opposite to keep the cross section or the outer perimeter constant-, decreasing the mass flow rate per tube and, with it, its velocity.

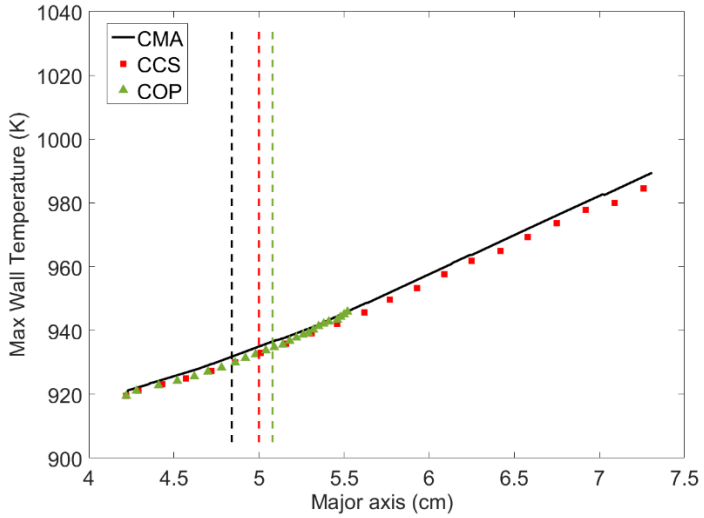

FIGURE 5. Maximum wall temperature.

However, radiation losses, which depend both on the tube's wall temperature fourth power and the view factor, decrease the greater the axis ratio becomes, meaning that the tube-sky interaction play the most important part in said losses. This becomes especially obvious when comparing the circular case and the elliptical with the same outer perimeter (COP): the radiative surface is the same, but yet the losses are significantly lower, Figure 6.

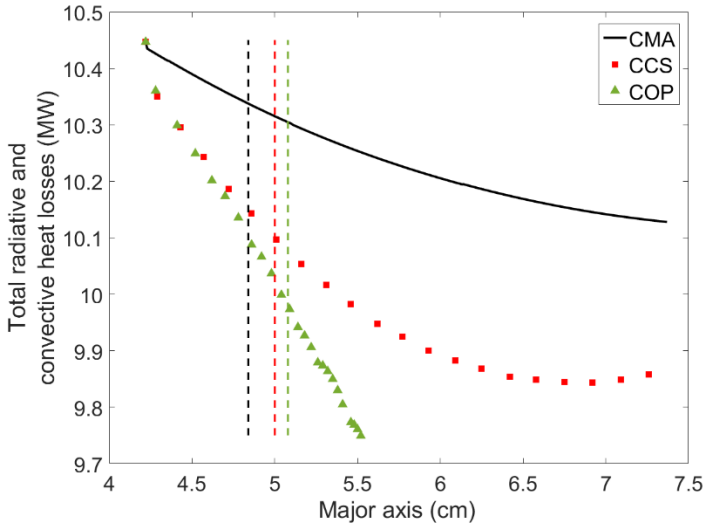

FIGURE 6. Total heat losses due to radiation and convection.

The evolution of the aggregation of radiation and external convection losses for the whole receiver is shown in Figure 6. External convection heat losses increase in all the receiver's tubes with the major axis length, since the outer surface does the same (in CMA and CCS cases) as well as the wall temperature of the tube -and both are key factors for convective losses-, but before the optimum efficiency is reached, such losses are not enough to counteract the decrease of the radiation heat losses; the sum of both losses has a decreasing tendency for the first values of the set of major axis tested. Once the minimum has been reached, the increase of the external convection losses has enough entity to counteract the decrease of the radiation heat losses, increasing progressively the aggregation of both of them with the major axis, being this the explanation for the efficiency decrease.

Comparing the results obtained for the three elliptical tubes it can be seen that the most favourable one is the instance having the same outer perimeter (COP). This seems reasonable since, to keep the outer perimeter constant while increasing the major axis, the cross section decreases. A lower cross section means a higher salt velocity, counteracting the effect of the increase in the number of tubes and implying a slightly better tube-salt heat transfer coefficient that, considering as well the influence of the view factors, make this the best alternative. On the other hand, the advantage of the decrease of the salt's velocity in the other two cases is that the total pressure drop of the tubes decreases (Fig. 7), since it depends on the square of the velocity, although this decrease becomes the most obvious for major axis values where the maximum film temperature allowable is surpassed. Therefore, even though the COP doesn't provide much of an advantage in this aspect when it is compared with the other two cases, the pressure drop is still lesser than in the circular case. This improvement in the pressure drop allows to reduce the plant's self-consumption and opens the possibility to study the increase of the receiver's number of panels to increase its thermal power while maintaining the total pressure drop.

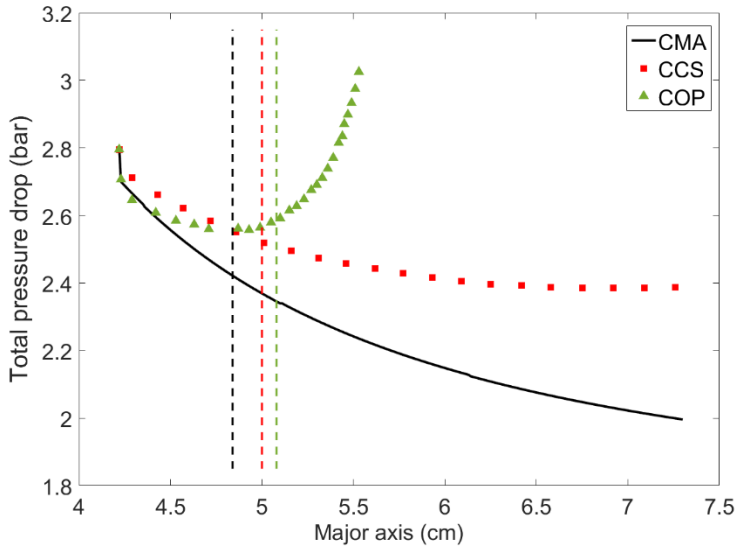

FIGURE 7. Total pressure drop vs the tube's major axis for the three cases considered.

CONCLUSIONS

Using elliptical tubes in the receiver results in the decrease of the energy irradiated to the surroundings from the tubes, due to the importance that the view factors pay on that issue. This translates in lesser radiative heat losses and, consequently, in a better receiver's thermal efficiency, allowing a more precise sizing of the heliostats field and decreasing the installation costs. The cross section and the number of tubes are relevant aspects on the efficiency since they affect the salts velocity, which has a huge importance on the heat transference from the tubes to the salts, and therefore the tube's wall temperature.

Maintaining constant the outer perimeter happens to be the best option out of the ones studied from the efficiency point of view, since it results in the lesser interaction with the sky and the increase of the number of tubes with the major axis is counteracted with the decrease in the cross section, always paying attention to the total pressure drop. Overall, there is a decrease in the salt's velocity, resulting in lesser pressure drops than in the circular tubes, improving

the plant's self-consumption, although it increases the tube's wall temperature, a negative aspect that cannot be avoided.

ACKNOWLEDGMENTS

This study has been supported and financed by the Iberdrola España foundation under the program "Ayudas a la investigación en energía y medio ambiente" and by the Spanish Economy and Competitiveness Ministry under the project ENE2015-69486-R (MINECO/FEDER, UE).

REFERENCES

1. The Power to Change: Solar and Wind Cost Reduction Potential to 2025, IRENA (Int. Renew. Energy Agency), June 2016.
2. Z. Liao, X. Li, C. Xu, C. Chang, Z. Wang, Allowable flux density on a solar central receiver, Renew. Energy 62 (2014), 747-753.
3. M.R. Rodríguez-Sánchez, A. Soria-Verdugo, J.A. Almendros-Ibáñez, A. Acosta-Iborra, D. Santana, Thermal design guidelines of solar power towers, Appl. Therm. Eng. 63 (2014), 428–438.
4. J.M. Lata, M. Rodríguez, M. Álvarez de Lara, High Flux Central Receivers of Molten Salts for the New Generation of Commercial Stand-Alone Solar Power Plants, Journal of Solar Energy Eng. 130 (2008).
5. N. Boerema, G. Morrison, R. Taylor, G. Rosengarten, Liquid sodium versus Hitec as a heat transfer fluid in solar thermal central receiver systems, Solar Energy, 86 (2012), 2293–2305.
6. M.R. Rodríguez-Sánchez, A. Sánchez-González, D. Santana., Feasibility study of a new concept of solar external receiver: Variable velocity receiver, Applied Thermal Engineering 128 (2018), 335-344
7. G. J. Kolb. An Evaluation of Possible Next-Generation High-Temperature Molten-Salt Power Towers. Sandia Report SAND2011-9320, December 2011
8. N. Boerema, G. Morrison, R. Taylor, G. Rosengarten, High temperature solar thermal central-receiver billboard design, Solar Energy 97 (2013), 356–368
9. M. Yang, X. Yang, X. Yang, J. Ding, Heat transfer enhancement and performance of the molten salt receiver of a solar power tower, Appl. Energy 87 (2010), 2808-2811.
10. O. Garbrecht, F. Al-Sibai, R. Kneer, K. Wieghardt, CFD-simulation of a new receiver design for a molten salt solar power tower, Sol. Energy 90 (2013), 94-106.
11. Z. Liao, A. Faghri. Thermal analysis of a heat pipe solar central receiver for concentrated solar power tower, Applied Thermal Engineering 102 (2016), 952–960
12. M.R. Rodríguez-Sánchez, A. Sánchez-González, C. Marugán-Cruz, D. Santana, New designs of molten-salt tubular-receiver for solar power tower, Energy Procedia 49 (2014), 504 – 513
13. D. Santana Santana, M.R. Rodríguez Sánchez, M. Laporte Azcué, J. López Puente, A. Acosta Iborra, "Receptor solar de torre exterior", ES Patent P201830587, 15/06/2018.
14. M.R. Eslami, R.B. Hetnarski, J. Ignaczak, N. Noda, N. Sumi, Y. Tanigawa, Theory of elasticity and thermal stress: explanations, problems and solutions, 1st ed., Springer Sci and Business Media, Dordrecht, 2013.
15. A. Montoya, M.R. Rodríguez-Sánchez, J. López-Puente, D. Santana, Thermal and mechanical stresses in a solar central receiver, Renewable energy and Power Quality Journal, vol 1 (2018), No. 16.
16. A.B. Zavoico, Solar Power Tower, Design Basis Document, San Francisco, 2001.
17. A.M. Kruizenga, D.D. Gill, M. LaFord, J. McConohy, Corrosion of high temperature alloys in solar salt at 400, 500, and 680 ºC. Sandia National Laboratories, SAND 2013-8256, Albuquerque, Sept 2013
18. V.M.B. Nunes, C.S. Queirós, M.J.V. Lourenço, F.J.V. Santos, C.A. Nieto de Castro, Molten salts as engineer ing fluids – A review. Part I. Molten alkali nitrates, Applied Energy 183 (2016), 603-611.
19. M.R. Rodríguez-Sánchez, A. Sánchez-González, C. Marugán-Cruz, D. Santana, Flow patterns of external solar receivers, Solar Energy 122 (2015), 940-953.
20. A. Sánchez González, D. Santana. Solar flux distribution on central receivers: a projection method from analytic function. Renew. Energy 74 (2015), 576-587
21. D. Cain, A. Roberts, H. Barrow, An experimental investigation of turbulent flow and heat transfer in elliptical ducts. Wärme und Stoffübertragung 2 (1973) 101-107.
22. M.F. Modest, Radiative heat transfer, 2nd ed., Elsevier Science, USA, 2003, pp. 131-161.